COHESIVE STRENGTH IMPROVEMENT MECHANISM OF KAOLINITE NEAR THE ANODE DURING ELECTROOSMOTIC CHEMICAL TREATMENT

Yuan-Shiang Lin[1], Chang-Yu Ou[1],*, and Shao-Chi Chien[2]

[1] Department of Civil and Construction Engineering, National Taiwan University of Science and Technology, No. 43, Sec. 4, Keelung Rd., Taipei City 10607, Taiwan
[2] Aletheis University, No.32, Zhenli St., Danshui Dist., New Taipei City 25103, Taiwan

Abstract—Injection of $CaCl_2$ and Na_2SiO_3 solutions into clay suspensions during electroosmosis often improves the cohesive strength of clays near the anode and cathode, whereas the cohesive strength of clays between the electrodes remains weak. Although the main improvement mechanism for the cohesive strength of clays near the cathode was demonstrated to be a pozzolanic reaction (formation of calcium silicate hydrate cement), the mechanism of improved cohesive strength near the anode is still not understood. The objective of the present study was to investigate the mechanism for the improvement of cohesive strength near the anode and, thus, make it possible to determine a way to enhance the range in improvement using kaolinite as the test clay. The test was performed by first injecting $CaCl_2$ solution during electroosmosis until the optimum volume of $CaCl_2$ was attained. This was followed by treatment with Na_2SiO_3 solution for different lengths of time. The results indicate that the anode region after treatment was acidic (pH = 4) because the electrolysis of water causes acidification near the anode. As Na_2SiO_3 solution was injected through the anode, the mechanism of cohesive strength improvement of the treated clay near the anode was attributed to the silicic acid polymerization effect provided by the Na_2SiO_3 solution. The silicic acid may link the clay particles together to form a gel network in a low pH environment. The clay gel network structure developed rigidity as the water content was reduced. In addition, as the volume of injected Na_2SiO_3 solution was increased, the cohesive strength near the anode also increased.

Key Words—Anode Area, Electrokinetic Treatment, Electroosmotic Chemical Treatment, Polymerization.

INTRODUCTION

Electroosmotic chemical treatment (ECT), also called electrokinetic treatment, is a technique that combines electroosmosis and the injection of chemical solutions to improve the strength of clays in order to stabilize building foundations and prevent slope failure or soil erosion (Rogers *et al.*, 2003). When a moderate electrical potential gradient is applied to a saturated clay, the pore water will move from the anode to the cathode. Simultaneously, chemical solutions can be injected into the treated clay either through the anode or cathode using the combined electrical and hydraulic flows across the clay. The chemical reaction from this process cements the clay particles together, which enhances the permanent stability of the clay suspension. The results of the ECT test vary with different combinations of injected solutions and treatment durations.

The ECT process has been studied by Ou and coworkers (*e.g.*, Ou *et al.*, 2009, 2013, 2015; Lin *et al.*, 2017) as well as by many other investigators (*e.g.*, Otsuki *et al.*, 2007; Nordin *et al.*, 2013; Mosavat *et al.*, 2013). Many types of chemical additives have been injected during the ECT process. Calcium chloride ($CaCl_2$) and Na_2SiO_3 solution, which have the noticeable advantages of being non-toxic, non-contaminating, and of low cost, have frequently been used as an injection material and published research has shown that $CaCl_2$ and Na_2SiO_3 solutions applied during the ECT process effectively improves the cohesive strength of the clay (*e.g.*, Liaki *et al.*, 2007, 2008, 2010; Abdullah and Al-Abadi, 2010; Nordin *et al.*, 2013; Ou *et al.*, 2013; Mosavat *et al.*, 2013). The improvement range found in the studies mentioned above, however, was mostly limited to the areas near to either the anode or the cathode. If the mechanism of cohesive strength improvement near the anode and cathode can be understood, extension of the improvement range throughout the entire sample may be feasible by adjustments in the injection procedure or by the use of another new injection solution.

Ou *et al.* (2015) found that the improvement mechanism of the clay near the cathode is related to a pozzolanic reaction (*i.e.* particles bound together by the formation of calcium silicate hydrate cement) when $CaCl_2$ and Na_2SiO_3 solutions were injected through the anode, which is consistent with other published reports (Barker *et al.*, 2004; Asavadorndeja and Glawe, 2005; Ahmad, 2012). The pozzolanic reaction occurs when injected Ca^{2+} ions react with dissolved Al and Si from

clays in an alkaline environment, which causes calcium silicate and/or calcium aluminate hydrate formation. The calcium silicate and/or calcium aluminum hydrates are described as C-S-H and C-A-H gels, respectively, in cement chemist notation. The formation of these gels cements the clay particles together and increases the cohesive strength of the clay.

Moreover, a significant improvement in the cohesive strength of the clay that surrounds the anode is also observed when a Na_2SiO_3 solution is injected through the anode. The mechanism of improvement can be attributed either to the formation of new compounds within the clay particle structure or to cementation agents that bind the clay particles together. According to the chemical reaction between the Na_2SiO_3 and the clay particles, the cementing agents can either be calcium silicate hydrate or calcium aluminate hydrate that result from pozzolanic reactions or to the polymerization of silicic acid from the Na_2SiO_3 solution as noted by Iller (1979). These cementing agents, however, cannot be detected easily because the cementing agents have amorphous characteristics and the existence of the cementing agents can be confirmed only by inference from the relevant chemical reactions.

The objective of the present study was, therefore, to study the key cementation mechanism near the anode area by injecting $CaCl_2$ and Na_2SiO_3 solutions during the ECT process and to observe electroosmosis, electromigration, and other electrochemical effects on the physical and chemical behavior of the treated clay.

After understanding the cementation mechanism near the anode, a more effective method may be developed in the future to extend the improved cohesive strength range to the whole treated sample.

MATERIALS AND METHODS

An ECT cell, originally designed by Ou *et al.* (2013), was used in this study (Figure 1). The cell consisted of three different parts: the top part, the rectangular model tank, and the bottom plate. The top part was used to transfer stress to the clay specimen during consolidation. The rectangular model tank was composed of a nonconductive transparent Plexiglas® sheet with a thickness of 45 mm. The main compartment had internal dimensions of 350 mm × 150 mm × 250 mm. Two small compartments with internal dimensions of 20 mm × 150 mm × 170 mm were used to inject chemical solutions and to drain off water. The bottom plate had four holes for water drainage during consolidation and was fitted with three Ti sensors to record variations in the voltage during the ECT tests.

The ECT test was conducted in two main phases as shown in Table 1. During Phase 1, $CaCl_2$ solution was injected through the anode for a long period of time (168 h) to estimate the turning point, *i.e.*, the most suitable length of time to supply $CaCl_2$ solution during the ECT test. This test was designated C168. Phase 2 was performed by first injecting the $CaCl_2$ solution
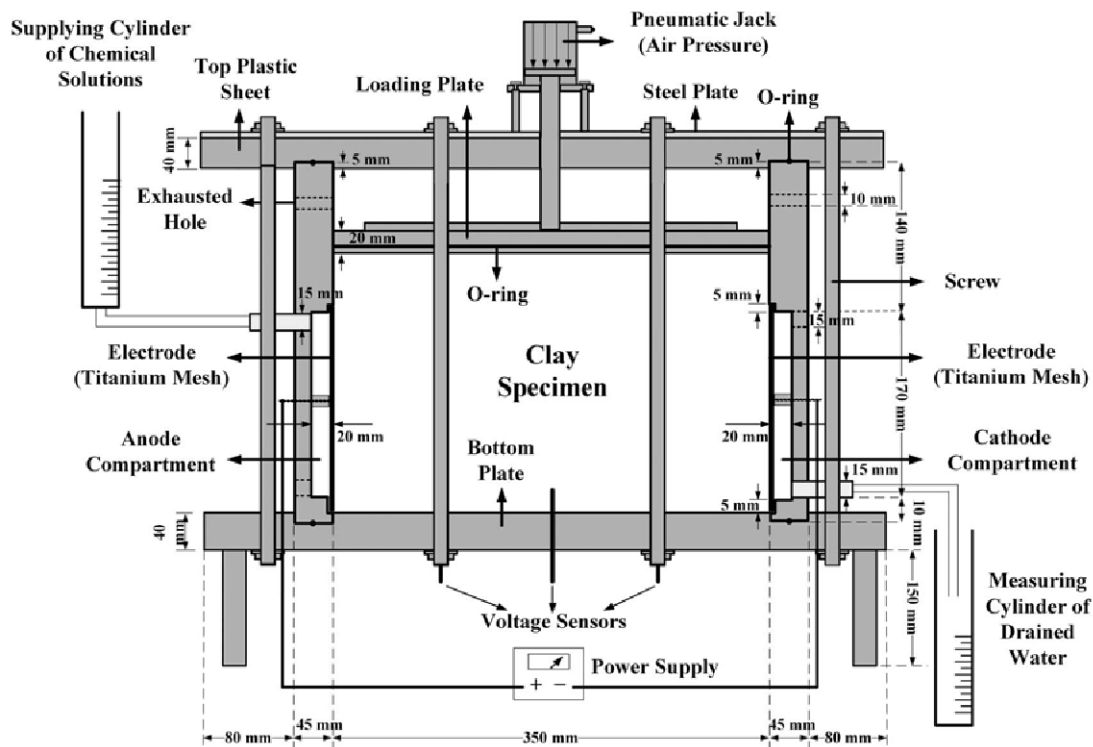

Figure 1. Schematic diagram of ECT test cell showing side view (Ou *et al.*, 2013).

Table 1. The main ECT test program.

Test	– Duration (h) –		Total duration (h)
	CaCl$_2$	Na$_2$SiO$_3$	
Phase 1			
1. C168	168	–	168
Phase 2			
1. C72N72	72	72	144
2. C72N144	72	144	216

Table 3. Engineering properties of the kaolinite used in this study (Chang *et al.*, 2010).

Physical properties	Value
Liquid Limit (%)	46
Plastic Limit (%)	25
Plastic Index (%)	21
Specific Gravity (g/cm^3)	2.61
Particle Size (μm)	1.0−2.0
pH	6~8
Specific Surface Area (m^2/g)	24
Natural Water Content (%)	1
Classification	CL

through the anode until the turning point, followed by treatment with Na$_2$SiO$_3$ solution for different lengths of time through the anode. This test was designated C72Nyy. In the test designations, the symbol "C" represents CaCl$_2$ solution, "N" represents Na$_2$SiO$_3$ solution (Produced by PQ Corporation, Malvern, Pennsylvania, USA, with Na$_2$O/SiO$_2$ = 3.15, specific gravity = 1.34) and "yy" is the length of the treatment in hours when Na$_2$SiO$_3$ solution was used. As listed in Table 1, the total C72N72 ECT treatment duration was 144 h and the total C72N144 ECT treatment duration was 216 h.

The test clay was an unpurified kaolinite sample supplied by U.S. Silica Company from Warren County, Georgia, USA, with a cation exchange capacity of 3.4 cmol/kg. The chemical compositions and engineering properties of the kaolinite are shown in Tables 2 and 3, respectively. The kaolinite powder was thoroughly mixed with a sufficient amount of distilled deionized water using a mechanical mixer so that the water content was 60%. The clay slurry was placed into the test container one layer at a time in three layers of equal thickness. After placing the clay into the ECT cell, a filter paper was placed on top of the clay and the electrodes (Pt-coated Ti mesh) were attached. The test samples were then prepared by applying an axial stress (*i.e.* vertical) of 15 kPa for approximately 1 d and then at 30 kPa for 3 d. Then, during the ECT test, the applied axial stress was maintained at 30 kPa. After consolidation, the piezometers and voltage sensor were connected to the ECT cell. Finally, the direct current (DC) power

supply was connected to both sides of the electrodes.

The sequence of injections included 3 different tests as described previously. The CaCl$_2$ solution concentration used in this test was 0.75 M based on the study by Chang *et al.* (2010) and the Na$_2$SiO$_3$ solution concentration was set at a 1:1 volume ratio (Na$_2$SiO$_3$ / deionized water) according to Ou *et al.* (2013). All of the chemical solutions were injected from the anode only. The injection procedure was subject to a constant applied voltage of 17.5 V (0.05 V/mm), which is an optimum voltage gradient for geotechnical purposes as suggested by Mitchell and Soga (2005).

The cohesive strength of the treated clay was tested using a specially designed laboratory cone penetration apparatus, which was attached to an adjustable rod that was 9.2 mm in diameter (Figure 2). The test procedure followed the *ASTM D5778-12* procedure (ASTM D5778-12, 2012), in which the penetration rate was 2 cm/s. The cohesive strength of the clay was measured at 5 locations

Table 2. Chemical composition (wt.%) of the kaolinite used in this study (Chang *et al.*, 2010).

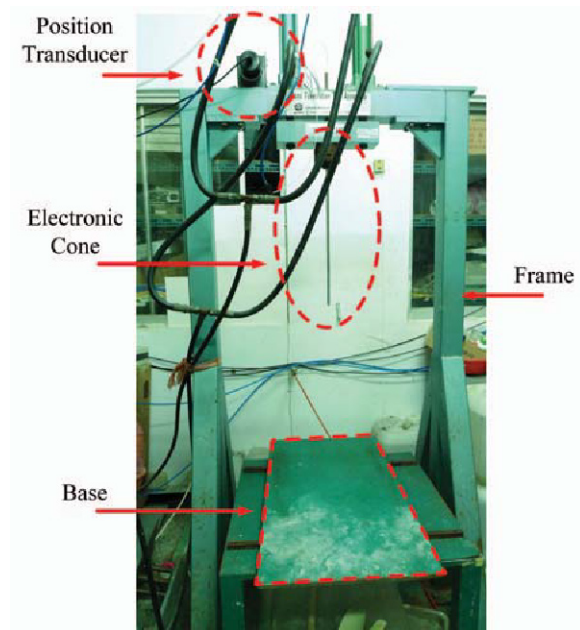| Chemical analysis	Mean percentage
SiO$_2$	44.5
Al$_2$O$_3$	39.5
TiO$_2$	1.0
MgO	0.07
Na$_2$O	0.52
Fe$_2$O$_3$	0.5
CaO	0.05
K$_2$O	0.04
Loss On Ignition	13.6

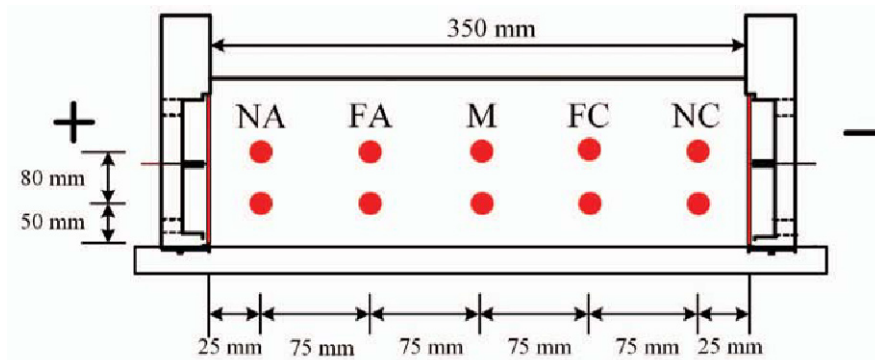Figure 2. Photo of cone penetration test (CPT) device.

Figure 3. Side view of the CPT test and the NA, FA, M, FC, and NC water content measurement locations.

along the depth of the sample between the anode and the cathode: NA (near the anode), FA (far from the anode), M (middle part), FC (far from the cathode), and NC (near the cathode) (Figure 3). Only the NA data were presented for the discussion of the cementation mechanism at the NA location. The cohesive strength of the clay in the present study was, therefore, measured as the cone resistance (q_c).

After the completion of the cone penetration test (CPT) the water contents of the treated clay (Figure 3) were measured at 10 locations between the anode and the cathode according to the *ASTM D2216-10* procedure (ASTM D2216-10, 2010). The clay pH values were measured using dried clay samples after the water contents were measured. According to the *ASTM D4972-13* procedure (ASTM D4972-13, 2013), 10 g of dried clay samples (ground to <2 mm diam) were first thoroughly blended with 10 mL of deionized water in a centrifuge tube. Then, the water in the clay slurry samples was drained off using a centrifuge and the pH values of the liquid were measured using a pH meter.

Concentrations of Ca^{2+} were measured using a Horiba JY 2000-2 inductively coupled plasma atomic emission spectrometer (ICP-AES) (Horiba Scientific, Kyoto, Japan). The tested samples, according to the *ISO 11466* procedure (ISO 11466, 1995), should be digested in 10 mL of aqua regia solution (3:1 volume ratio of 35% HCl to 69% HNO_3) for 24 h and then heated on a hotplate at 130ºC for 2 h. The suspensions were then filtered using a membrane filter (0.22 μm) at room temperature, diluted with 100 mL of 0.5 M HNO_3, and stored in polyethylene bottles for analysis.

X-ray diffraction (XRD) using a Bruker D2 Phaser X-ray diffractometer (Bruker AXS Gmbh, Karlsruhe, Germany) was used to determine the phases in a specimen by comparing the patterns to patterns in the JCPDS (Joint Committee on Powder Diffraction Standards) database. The samples were scanned using CuKα radiation from 15º to 70º2θ with a step size of 0.05º2θ and a scan speed of 1 s/step.

Solid-state ^{29}Si NMR using a Varian Infinity^{plus} 400 MHz instrument (Varian, Palo Alto, California, USA) was used to determine the bonding of the silica gel to the treated clay. The bonding structure between the Si atoms was denoted by Q^m. The values of *m* ranged from 0 to 4 and indicate the weakest (0) to the strongest (4) bonding as shown in Table 4.

To understand the effects of the chemical solution treatments, the water contents, pH values, XRD patterns, NMR spectra, and cone penetration resistance values

Table 4. Chemical shift and structure in analysis using solid state ^{29}Si NMR spectroscopy (Davidovits, 2008).

Symbol	Q^0	Q^1	Q^2	Q^3	Q^4
Chemical shift δ (ppm)	−66~−73	−76~−83	-86~−91	−95~−101	−103~−120
Chemical structure	H O | HO−Si−OH | O H	H O | HO− | Si−O−Si O H	H O | Si−O | Si−O−Si O H	Si | O | Si−O−Si−O−Si | O H	Si | O | Si−O−Si−O−Si | O | Si
Appellation	Monosilicate	Disilicate	Linear silicate	Grafted silicate	3-D silicate

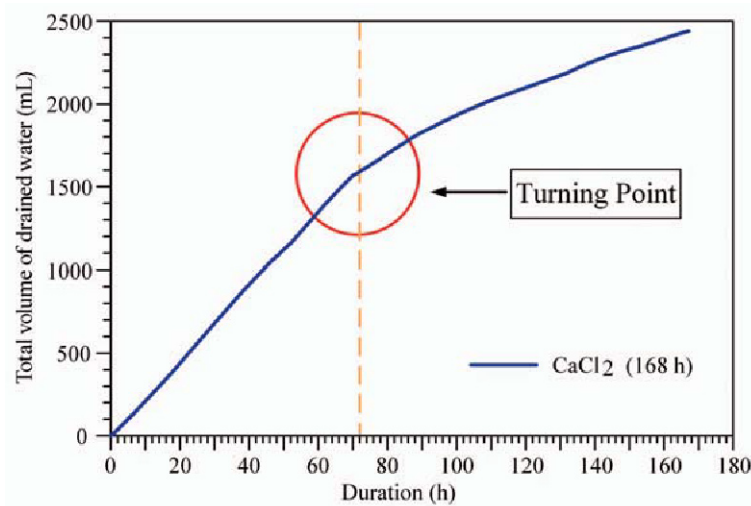Figure 4. The total volume of drained water plotted *vs.* test duration while CaCl$_2$ solution was injected.

were measured on specimens with and without chemical solution treatments after the full consolidation regime in the ECT cell at the same vertical pressure. The control test specimens without chemical solution treatments were termed as "untreated" in this study.

RESULTS

Turning point

After CaCl$_2$ solution was injected into a clay sample for several h, an inflection point was reached in the slope of a plot of injection duration time *versus* total volume of water drained from the cathode. This inflection point is called the "turning point." According to Ou *et al.* (2013), the turning point can be taken as the most suitable time to change to another injection solution. The test results (Figure 4) of the present study indicated that the turning point was 72 h. When the injection duration was longer than the turning point, an amorphous calcium silicate hydrate gel was formed between the clay particles near the cathode. This slowed the electro-osmosis process, prevented water from draining off, and decreased the volume of the Na$_2$SiO$_3$ solution that was subsequently injected (Figure 4).

Cone resistance

The variation in clay cone resistance (q$_c$) values with depth (*i.e.*, vertical direction) at the NA (near anode) position (Figure 5) revealed that the clay treated only with the CaCl$_2$ solution (*i.e.*, C72) exhibited only a small (350 kPa) improvement in cone resistance near the anode, which was about 2.3 times greater (150 kPa) than that for the untreated condition. The cone resistance of the clay at the NA position increased remarkably, however, with continuous injection of Na$_2$SiO$_3$ solution. A greater Na$_2$SiO$_3$ solution treatment duration resulted in a greater increase in cone resistance. The average

cone resistance value grew as the injected volume of the Na$_2$SiO$_3$ solution was increased (Figure 6). The final cone resistance value after treatment ranged from 2 to 5 MPa and the greatest cone resistance occurred in the anode region. With such a high cone resistance value for the treated clay, the increased cone resistance was attributed to a combination of the formation of new compounds and/or cementing agents, a change in the clay properties, and/or a reduction in the water content. The aim of the experimental regime reported, henceforth, was to clarify the strengthening mechanisms.

Water content

The water content measured from the anode to the cathode across the clay samples (Figure 7) indicated that the water content after treatment mostly decreased to values less than those in the untreated condition (*i.e.*, 51%), except for clay samples in the NC region. The water content basically decreased with treatment duration, especially near the NA region. This trend may have been due to the fact that the injection of CaCl$_2$ would flocculate the clay, which in turn increased the permeability of clay. The CaCl$_2$ and Na$_2$SiO$_3$ solutions would also increase the electrical conductivity and the amount of cations, which would cause more water to migrate towards the cathode. The water content, thus, increased with increased distance from the anode and decreased with greater treatment duration.

pH measurement

The pH values measured across the clay samples (Figure 8) indicated that the pH values in the anode region decreased significantly to pH 4 after treatment. The change in pH values in this region should be due to the electrolysis of water only rather than to the release of ions from the anode because Pt-coated Ti electrodes were used in this study. The phenomenon was similar to treatments
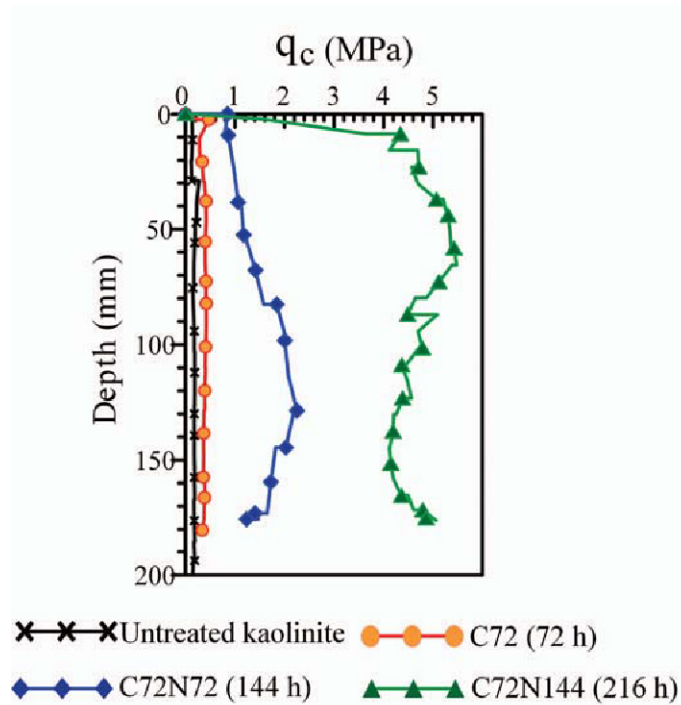
Figure 5. Plot of CPT resistance *vs.* cone resistance (q_c) near anode area (NA) in Phase 2 of experiments for the untreated clay and treated samples C72, C72N72, and C72N144.

that used inert electrodes (Liaki *et al.*, 2007, 2008), but different from treatments that used steel or stainless steel where Fe ions may have been released from the anode during electroosmosis (Rogers *et al.*, 2003; Liaki *et al.*, 2007, 2010). Conversely, near the cathode, the pH increased considerably to approximately 9 or 10 after a longer treatment duration and indicated the creation of an alkaline environment from the generation of hydroxyl ions from the electrolysis of water at the cathode.

Moreover, with an increase in the Na_2SO_3 solution treatment duration, the alkaline front moved toward the middle part of the sample from the cathode. This may be due to the fact that part of the hydroxyl ions from the injection of Na_2SO_3 solution were brought toward the cathode by electroosmotic flow rather than being from the hydroxyl ions that were generated at the cathode and moved toward the anode. In addition, the pH in the middle part of the treated clay was neutral because the hydrogen
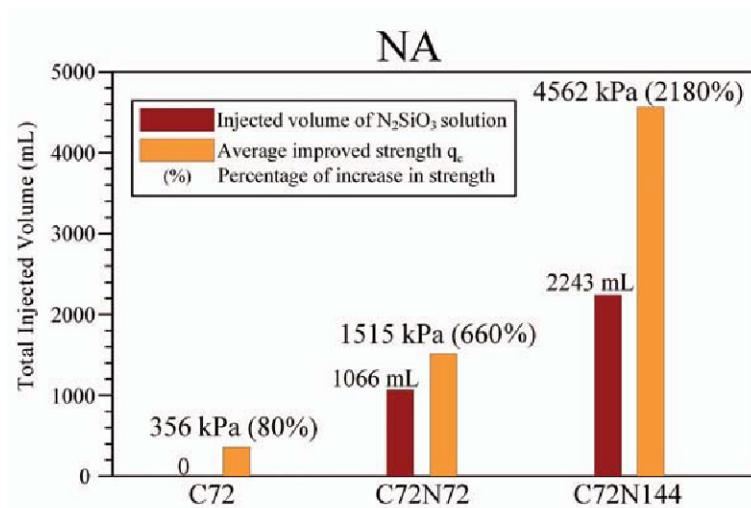

Figure 6. The relationship between average CPT resistance and injected volume of Na_2SiO_3 solution in Phase 2 of experiment in NA region for the untreated clay and treated samples C72, C72N72, and C72N144.
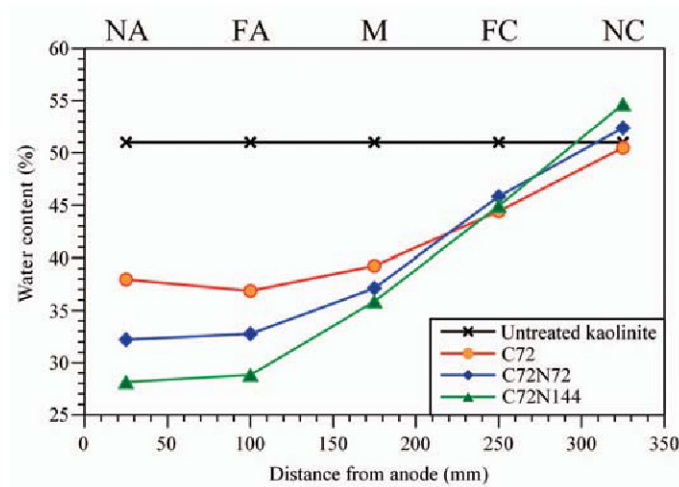
Figure 7. Plot of %water content *vs.* distance from the anode in Phase 2 of the experiments for untreated clay and treated samples C72, C72N72, and C72N144

ions and hydroxyl ions moved toward the cathode and anode, respectively. Both ions, thus, met at the middle part of the sample and the environment was neutralized as discussed by Liaki *et al.* (2008).

Concentration of Ca^{2+} ions

The concentrations of Ca^{2+} ions measured in the clay samples (Figure 9) included the Ca^{2+} ions adsorbed to the clay and Ca^{2+} ions in the pore water between clay particles. Figure 9 shows that Ca^{2+} ions first collected in the NA region at concentrations of approximately 25 ppm due to the constant injection of $CaCl_2$ solution through the anode. The Ca^{2+} ions then gradually migrated to the cathode through the processes of electroosmosis and electromigration and caused the Ca^{2+} to decrease from 25 to 10 ppm in the NA region.

When the Ca^{2+} ions migrated towards the cathode, $Ca(OH)_2$ would precipitate and accumulate in the alkaline environment in the FC and NC regions (Ou *et al.*, 2015). The amounts of Ca^{2+} were highly related to the pH values (Figures 8 and 9). The concentrations of Ca^{2+} ions detected in the FA and M regions, however, were almost the same as in the untreated clay where the pH values in the FA and M regions were almost neutral. This implies that only a very small amount of Ca^{2+} ions was in the pore water between clay particles and most Ca^{2+} ions in the FA and M region were adsorbed to the clay.

XRD analysis

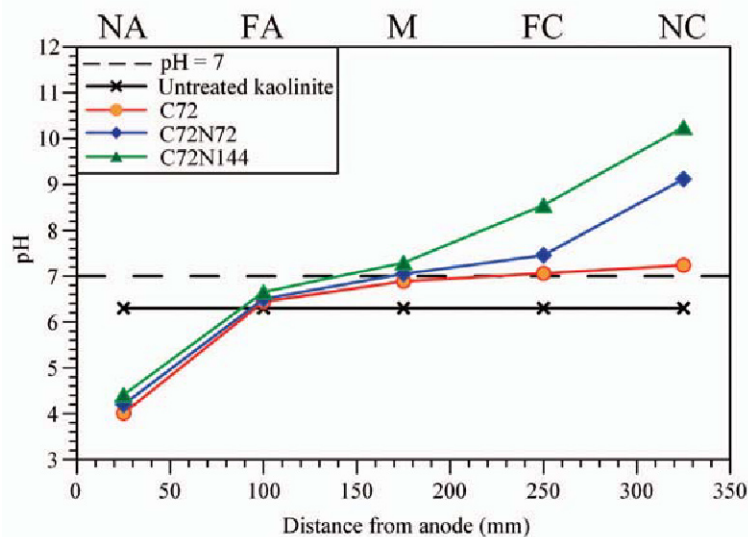The XRD analysis (Figure 10) showed no new peak in the pattern of specimen C72. The patterns of

Figure 8. Plot of pH values *versus* distance from the anode in Phase 2 of the experiments at pH = 7 and for the untreated clay and treated samples C72, C72N72, and C72N144.
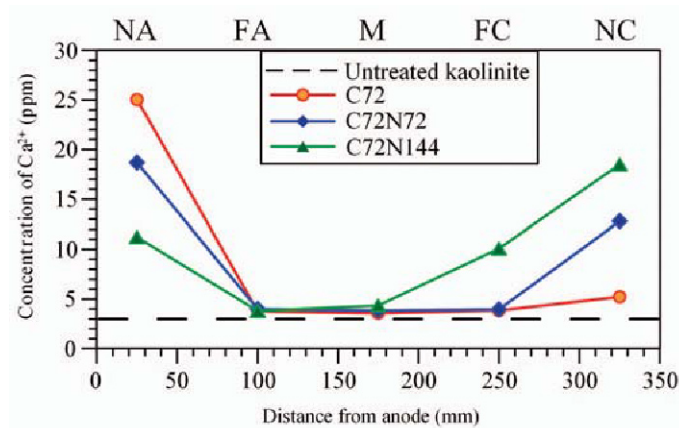
Figure 9. Plot of Ca^{2+} concentration *vs.* distance from the anode in Phase 2 of the experiments for untreated clay and treated samples C72, C72N72, and C72N144.

specimens C72N72 and C72N144, however, had a new peak at approximately 32º2θ and peaks at 26 and 46º2θ that had greater intensities than in the untreated kaolinite specimen. Comparing the XRD mineralogical analysis to the JCPDS database identified the 26º2θ peak as quartz (SiO_2) and the 32º2θ and 46º2θ peaks as NaCl. The quartz peak was also present in the untreated kaolinite, but the NaCl peaks were new after treatment. The NaCl peaks at 32º and 46º2θ in the test samples were also found in the XRD pattern of a dried mixture of $CaCl_2$ and Na_2SiO_3 solutions (Figure 10a).

The XRD pattern in Figure 10a was collected from a specimen prepared from a dried mixture of the $CaCl_2$ and Na_2SiO_3 solutions, which was prepared to characterize the mineral composition without the clay. This was to see if the ECT test might induce a chemical reaction between the $CaCl_2$ and Na_2SiO_3 solutions injected near the anode. This comparison, therefore, makes possible more correct deductions regarding the reason for the additional XRD peak.

NMR analysis

The results of the NMR analysis (Figure 11) indicated one strong peak at −91 ppm, a chemical shift in the range from −86 to −100 ppm consistent with a Q^2 structure (*i.e.* linear silicate) according to Davidovits (2008). The silica structure in the treated kaolinite was still linear and the NMR peak remained in the −86 to −100 ppm range even if the time duration of the Na_2SiO_3 solution injection was increased and the cone resistance of the clay near the anode was increased accordingly.

DISCUSSION

For the clay that was treated with only the $CaCl_2$ solution (*i.e.* C72), the possible factors that may have improved the clay cone resistance included cations and anions released from the electrodes, new chemical compounds formed, pH changes, or water content changes (Liaki *et al*., 2007, 2008). Because inert
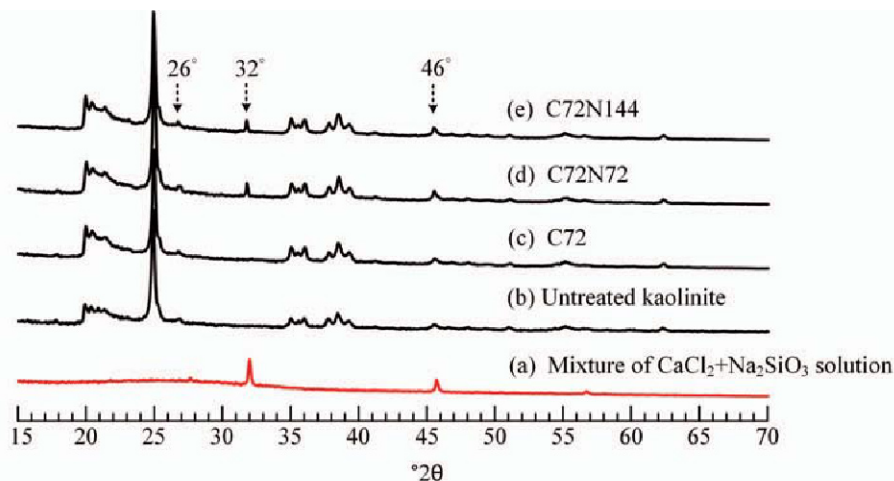

Figure 10. XRD patterns in the NA region for (a) Mixture of $CaCl_2$ + Na_2SiO_3 solution, (b) Untreated kaolinite, (c) C72, (d) C72N72, and (e) C72N144 samples.
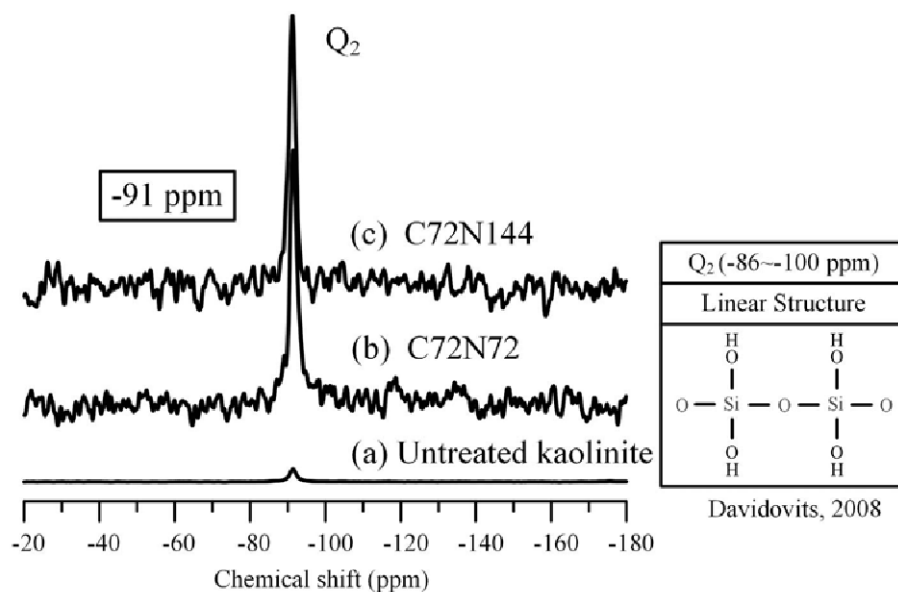
Figure 11. NMR patterns in Phase 2 of the experiments in the NA region for (a) untreated kaolinite, (b) C72N72, and (c) C72N144 samples.

electrodes (*i.e.* Pt-coated Ti electrodes) were employed in this study, the release of metal cations from the anode should have been eliminated. According to the XRD analysis (*i.e.* C72), no new chemical compounds or mineral phases were formed by the injection of Ca^{2+} ions only (Figure 10). A decrease in pH due to electrolysis of water and increase in the electrolyte concentration due to the injection of Ca^{2+} ions would decrease the thickness of the diffuse double layer and make clay particles flocculate. This in turn would increase clay cone resistance, but just within a small range (Liaki *et al.*, 2008). On the other hand, the injection of Ca^{2+} cations into clays in the electric field would increase the number of cations in the clay and result in an increase in electric conductivity and cations. More adsorbed water along with cations would, thus, migrate toward the cathode. A water content reduction of about 13% was found (Figure 7), which caused the untreated clay cone resistance to increase by about 2.3 times (Figure 5). With reference to the research of Liaki *et al.* (2008), the same reduction in the water content would increase the shear strength by about 4.5 times relative to the strength increase measured from the undrained control shear strength curve for English China Clay. Thus, the measured cone resistance increase in the present study could be explained by the decreased water content of the clay, which was basically an electroosmosis phenomenon with no chemical reaction between the clay particles.

The cone resistance of the clay near the anode was significantly improved for the clay treated with $CaCl_2$ solution followed by Na_2SiO_3 solution. In addition, a greater injection volume of Na_2SiO_3 solution resulted in a more effective increase in cone resistance near the anode.

As noted in the Introduction and Results sections, this cone resistance increase could be attributed to the reduced water content, the formation of new compounds within the 3-D chemical network structure, a calcium silicate hydrate/calcium aluminate hydrate (C-S-H/C-A-H) gel that results from a pozzolanic reaction, or the polymerization effects provided by silicic acid from the Na_2SiO_3 solution.

Similar to the mechanism for the $CaCl_2$ only treatment (*i.e.*, C72), the water content reduction was about 19% and 23% for the C72N72 and C72N144 tests, respectively. The corresponding cone resistance of the clay, however, increased to about 11 times and 30 times that of the untreated clay, respectively. Such a big increase in cone resistance would not only be due to the water content reduction, but it can be attributed to the formation of new chemical compounds or a cementing effect between particles.

The XRD analysis (Figure 10) indicated that only the crystalline phase of NaCl was identified as a new product, which should form by the reaction between the injected Na_2SiO_3 and $CaCl_2$ solutions in the NA region. The NMR analysis further identified intense peaks at −91 ppm (Figure 11) for C72N144 and C72N72 and a weak −91 ppm peak for kaolinite, which indicated that the silica chemical structure in the untreated and treated kaolinites was linear (Davidovits 2008) rather than three-dimensional. No newly formed chemical compounds contributed to the increased cone resistance of the clay.

Based on the pH measurements, the anode region was an acidic environment (pH = 4) after treatment (*i.e.* from hydronium ions generated by electrolysis of water). From the ICP-AES analysis, the Ca^{2+} ions first

accumulated in the NA region and then migrated to the cathode *via* electroosmosis and electromigration to an extent related to treatment duration. In a highly alkaline environment, silicate and aluminate will be released from the clay minerals and calcium silicate hydrate/calcium aluminate hydrate (C-S-H/C-A-H gel) may be formed if a sufficient amount of free Ca^{2+} cations are in the system (Barker *et al.*, 2004; Chang *et al.*, 2010; Ou *et al.*, 2015). The development of a C-S-H/C-A-H gel near the anode would not occur because the anode region was acidic. If this were the cause of the increased cone resistance, it would only occur in the NC region when the pH reached approximately 10. The C72N144 treatment was the only test in which this occurred (see Figure 8).

Because the increased cone resistance of the clay was not attributed to newly formed chemical compounds or to the C-S-H/C-A-H gel, it was not solely due to the effect of the reduced water content. The increased cone resistance was possibly only due to the silicic acid polymerization effect provided by the Na_2SiO_3 solution. This phenomenon can be explained using the schematic diagram in Figure 12, which is a famous and typical relationship between silicic acid gel time and pH (Iller, 1979). The sol with silicic acid in an acidic environment would speed up polymerization and achieve the gel point. This would cause small polymeric units of silicic acid to form a larger colloidal silica gel that would collide and link together into a branched network between the clay particles. The acidity (pH = 4) of the anode region and silicic acid polymerization between clay particles might be a clay cementation mechanism to improve clay properties by ECT near the anode. In addition, the decreased water content near the anode

could also contribute to the improvement and cause the gel network structure to become stronger after a longer period of treatment.

CONCLUSIONS

The mechanism of increased cone resistance near the anode was investigated after an injection of $CaCl_2$ solution was followed by an injection of Na_2SiO_3 solution during electroosmosis. After treatment, the clay environment near the anode was acidic and the only new crystalline phase detected using XRD analysis was NaCl. Additionally, the NMR spectra indicated that the silica chemical structure in treated kaolinite samples remained linear, which implies that no newly formed compounds contributed to the increase in clay cone resistance. A C-S-H/C-A-H gel could not develop near the anode because the anode region was acidic. In summary, the mechanism of clay improvement near the anode can primarily be attributed to the polymerization of silicic acid from the Na_2SiO_3 solution, coupled with the relatively smaller effect of a reduced water content. The silicic acid likely formed small colloidal particles in the low pH environment that linked together to form a gel network between clay particles. In addition, a greater volume of injected Na_2SiO_3 solution more effectively increased the cone resistance near the anode.

After the cone resistance improvement mechanism near the anode and cathode is fully understood, extending the improved cone resistance throughout the entire sample may be possible by adjusting the injection procedure or by using another new injection solution to change the pH of the entire sample.
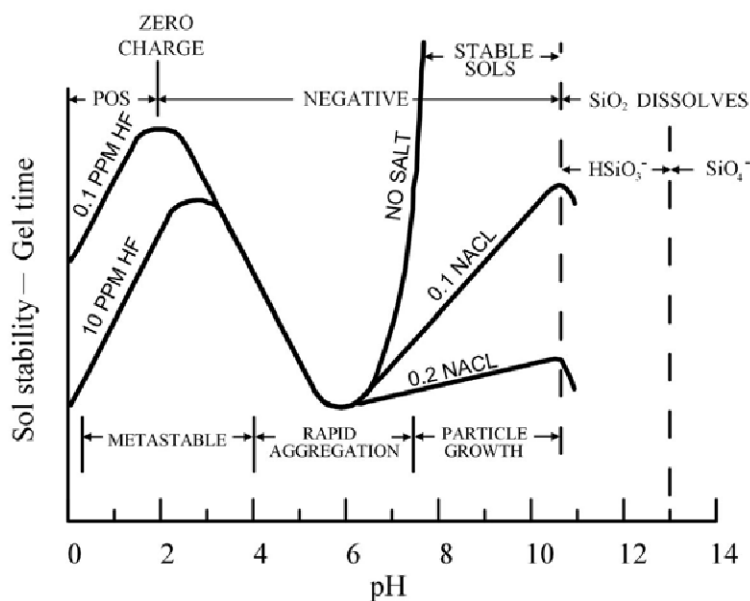

Figure 12. Relationship between silicic acid gel time and pH (Redrawn from Iller, 1979).

REFERENCES

Abdullah, W.S. and Al-Abadi, A.M. (2010) Cationic−electrokinetic improvement of an expansive soil. *Applied Clay Science*, **47**, 343−350.

Ahmad, T.S.A. (2012) *Electrokinetic Stabilisation of Soft Clay*. PhD thesis, School of Civil Engineering, University of Birmingham, UK.

Asavadorndeja, P. and Glawe, U. (2005) Electrokinetic strengthening of soft clay using the anode depolarization method. *Bulletin of Engineering Geology and the Environment*, **64**, 237−245.

ASTM D2216-10 (2010) *Standard Test Methods for Laboratory Determination of Water (moisture) Content of Soil and Rock by Mass.* https://www.astm.org/Standards/D2216.htm.

ASTM D4972-13 (2013) *Standard Test Methods for pH of Soils*. https://www.astm.org/Standards/D4972.htm.

ASTM D5778-12 (2012) *Standard Test Method for Performing Electronic Friction Cone and Piezocone Penetration Testing of Soils*. https://www.astm.org/Standards/D5778.htm.

Barker, J.E., Rogers, C.D.F., Boardman, D.I., and Peterson, J. (2004) Electrokinetic stabilization: An overview and case study. *Ground Improvement*, **8**, 47−58.

Chang, H.W., Krishna, P.G., Chien, S.C., Ou, C.Y., and Wang, M.K. (2010) Electro-osmotic chemical treatments: Effects of Ca^{2+} concentration on the mechanical strength and pH of kaolin. *Clays and Clay Minerals*, **58**, 154−163.

Davidovits, J. (2008) MAS-NMR spectroscopy. Pp. 70−78 in: *Geopolymer Chemistry and Applications*. 4th edition, Institute Géopolymère, Saint-Quentin, France.

Iler, R.K. (1979) *The Chemistry of Silica: Solubility, Polymerization, Colloid and Surface Properties and Biochemistry of Silica*. Wiley Interscience, New York.

ISO 11466 (1995) Soil quality − Extraction of trace elements soluble in aqua regia. https://www.iso.org/obp/ui/#iso:std:iso:11466:ed-1:v1:en.

Liaki, C., Rogers, C.D.F., and Boardman, D.I. (2007) Physico-chemical study of clay soil using inert and steel electrodes. *Proceedings of 6th International Symposium on Electrokinetic Remediation*, Vigo, Spain, 12th − 15th June.

Liaki, C., Rogers, C.D.F., and Boardman, D.I. (2008) Physico-chemical effects on uncontaminated kaolinite due to electrokinetic treatment using inert electrodes. *Journal of Environmental Health and Science - Part A*, **43**, 810−822.

Liaki C., Rogers, C.D.F., and Boardman, D.I. (2010) Physico-chemical effects on clay due to electromigration using stainless steel electrodes, *Journal of Applied Electrochemistry*, **40**, 1225−1237.

Lin, Y.S., Chien, S.C., and Ou, C.Y. (2017) On the improvement through the middle area of kaolinite with electroosmotic chemical treatment. *Journal of GeoEngineering*, **12**, 167−173.

Mitchell, J.K. and Soga, K. (2005) *Fundamentals of Soil Behavior*. 3rd Edition, John Wiley and Sons, New York.

Mosavat, N., Oh, E., and Chai, G. (2013) Laboratory assessment of kaolinite and bentonite under chemical−electrokinetic treatment. *Journal of Civil and Environment Engineering*, **3**, 1−7.

Nordin, N.S., Ahmad, T.S.A., and Abdul, K.A. (2013) Stabilisation of soft soil using electrokinetic stabilisation method. *International Journal of Zero Waste Generation*, **1**, 5−12

Otsuki, N., Yodsudjai, W., and Nishida, T. (2007) Feasibility study on soil improvement using electrochemical technique. *Construction and Building Materials*, **21**, 1046−1051.

Ou, C.Y., Chien, S.C., and Wang, Y.G. (2009) On the enhancement of electroosmotic soil improvement by the injection of saline solutions. *Applied Clay Science*, **44**, 130−136.

Ou, C.Y., Chien, S.C., and Lee, T.Y. (2013) Development of a suitable operation procedure for electroosmotic chemical soil improvement. *Journal of Geotechnical and Geoenvironmental Engineering, ASCE*, **39**, 993−1000.

Ou, C.Y., Chien, S.C., Yang, C.C., and Chen, C.T. (2015) Mechanism of soil cementation for electroosmotic chemical treatment. *Applied Clay Science*, **104**, 135−142.

Rogers, C.D.F., Liaki, C., and Boardman, D.I. (2003) Advances in the engineering of lime stabilised clay soils. *International Conference on Problematic Soils, Nottingham, UK*.